Research on Optical Spectrum Processing for Photonic-Assisted Broadband RF Cross-Eye Jamming System

Yunlu Xing, Shangyuan Li, Xiaoxiao Xue, and Xiaoping Zheng

***Abstract*—Cross-eye jamming technology has been used in electronic warfare, which attempts to protect a military platform from monopulse tracking radars. The cross-eye jamming technology has the ability of inducing angular errors to the monopulse tracking radars by transmitting two jamming signals with equal amplitudes and opposite phases. At present, high operation frequency and broadband cross-eye jamming system has been rarely demonstrated. Therefore, the present cross-eye jamming systems are hard to jam frequency-agile radar or multi-band radar, whose carrier frequency covers a large spectral range. In this paper, a photonic-assisted broadband radio frequency (RF) cross-eye jamming system is proposed and experimentally demonstrated. To achieve effective jamming effect, the intercepted radar signal is modulated to optical carriers and the phase shift is realized by optical spectrum processing. The relationship between system parameter tolerances and jamming effects are also simulated. Furthermore, the RF transfer function of X-band, Ku-band and K-band has been obtained in the experiments. The experimental results show that the amplitude and phase mismatch are below 2.15 degrees and 0.4 dB, respectively. Calculated cross-eye gain is 39 dB.**

***Index Terms*—Microwave photonic, cross-eye jamming, optical spectrum processing.**

I. Introduction

MONOPULSE tracking radars have the ability of measuring the direction of a target with a single pulse [1], [2]. Generally, four antenna beams are formed simultaneously to track the target in both pitching and azimuth direction. The angular location of the target is obtained by comparison of signal properties (phases or amplitudes) received by the different receivers. Compared with the direction of arrival (DoA) estimation algorithms [3], [4], [5], the computational cost of monopulse radar is lower. It takes little time to achieve the direction of the target because it requires just single pulse. Therefore, monopulse tracking radar has been widely used in missile guidance, target tracking and trajectory measurement, etc [6], [7], [8].

Manuscript received 28 December 2022; revised 19 March 2023; accepted 26 March 2023. Date of publication 7 April 2023; date of current version 13 April 2023. This work was supported by the National Nature Science Foundation of China under Grant 62127805. *(Corresponding author: Xiaoping Zheng.)*

The authors are with the Tsinghua National Laboratory for Information Science and Technology, Department of Electronic Engineering, Tsinghua University, Beijing 100084, China (e-mail: xingyl20@mails.tsinghua.edu.cn; syli@mail.tsinghua.edu.cn; xuexx@tsinghua.edu.cn; xpzheng@mail.tsinghua.edu.cn).

Digital Object Identifier 10.1109/JPHOT.2023.3263977

To improve the survivability of the combat aircrafts and ships, great efforts have been made to produce angular errors to monopulse radars. Researchers have proposed many angle deception jamming methods against monopulse radars, for example, cross-polarization jamming [9], [10], [11], formation jamming [12], [13], towed decoy [14], [15] and cross-eye jamming[16], [17], [18], [19], [20]. Among all these jamming methods, cross-eye jamming is regarded as the most effective jamming technology against monopulse radars [11].

To induce angular errors to monopulse radars, the cross-eye jammer creates two repeated radar signals which have equal amplitudes and opposite phases [21]. The two repeated radar signals distort the phase-front and an angular error is induced to the monopulse radar subsequently [22].

Various cross-eye jamming systems based on electrical technology have been published [23], [24], [25], [26], [27]. However, the electrical cross-eye jamming systems suffer severely from the limited bandwidth because of the electronic bottleneck. The broadband electrical phase shifters usually have non-uniform response over a wide frequency range. Although the proposed schemes can jam conventional electrical radar, they are hard to deal with microwave photonic radars with wide instantaneous bandwidth or frequency range. Based on photonic technology, X-band radar with 4 GHz bandwidth[28], K-band radar with 8 GHz bandwidth [29], [30] as well as Ka-band radar with 12 GHz bandwidth have been demonstrated [31]. For multi-band radar, even if the instantaneous bandwidth is narrow, the carrier frequency covers 10 GHz [32], [33].

To deal with these issues, photonic-assisted cross-eye jamming system have been proposed [34]. In [34], the two received radar signals are modulated to two Mach-Zehnder modulators (MZMs), respectively. And the two MZMs are operated at negative quadrature bias point and positive quadrature bias point, respectively. After photoelectric conversion, the two generated jamming signals are 180° out of phase. However, the jamming effect is subject to the low tuning accuracy.

We experimentally demonstrate a novel photonic-assisted cross-eye jamming system in this paper. The received radar signals modulate the optical carriers through MZMs. An optical spectrum processor (OSP) is used to ensure the repeated radar signals have the same amplitudes and opposite phases. Based on OSP, the control of the optical signals can be precise and flexible. The time delay of the two paths are also precisely tuned.

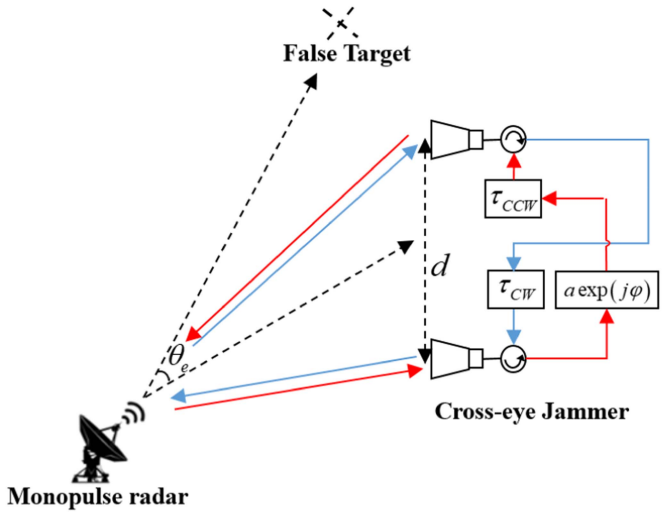

Fig. 1. General architecture for a cross-eye jammer.

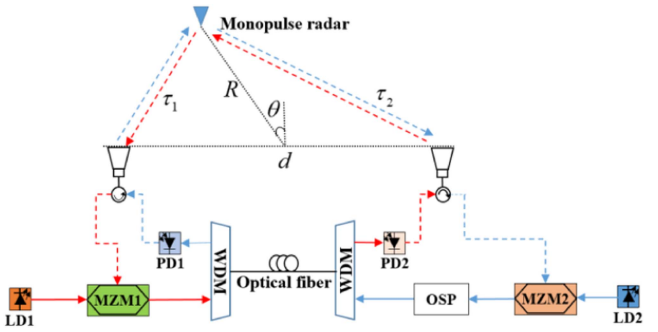

Fig. 2. Configuration of the novel photonic-assisted cross-eye jamming system. (b), (c) Optical spectrum before and after optical spectrum processing. LD: Laser diode; WDM: Wavelength division multiplexer; OSP: Optical spectrum processor; MZM, Mach-Zehnder modulator; PD: Photodetector.

Based on this principle, flexible phase shift can be achieved to compensate the phase deviation caused by the RF components or photoelectric devices. Thus, the tuning accuracy is higher than the technique in [34], which means higher cross-eye gain. After photoelectric conversion, the two jamming signals are generated. Compared with the traditional cross-eye jamming systems based on electrical methods, the novel photonic-assisted jammer has the ability of jamming the radars whose operating band covers a wide frequency band. Besides, fiber is used to replace the high-transmission loss and heavy coaxial cables to promote the capability of the proposed cross-eye jammer. The RF transfer function of X-band, Ku-band and K-band was measured in the experiment. The experimental results show that the amplitude mismatch and phase mismatch are lower than 2.15 degrees and 0.4 dB, respectively. Calculated cross-eye gain is 39 dB.

II. Principle

Fig. 1 shows a general architecture for a cross-eye jammer. The two repeated signals generated by the cross-eye jammer should maintain a phase difference of 180°, which means the cross-eye jammer is sensitive to rotation. In order to address this issue, cross-eye jammers should be retrodirective to ensure the two repeated radar signals transmit the same distance to the radar being jammed [22]. As indicated in Fig. 1, the cross-eye jammers usually use two opposite path to implement the retrodirective structure. τ_{CW} and τ_{CCW} are the transmission delays in CW (clockwise) and CCW (counterclockwise) directions, respectively. d is the distance between the two antennas. a and φ are the relative amplitude and phase difference of the two signals. To achieve high cross-eye gain and thus induce large angular error to the tracking radar, the two paths should have roughly equal amplitudes and time delays as well as ideally opposite phases ($a = 1, \tau_{CW} = \tau_{CCW}, \varphi = \pi$) [17]. Cross-eye jammer generates a false target. The combat platform and the false target are some distance apart, and θ_e is the angular error induced by the cross-eye jammer.

Based on this principle, we propose a novel photonic assisted cross-eye jamming system, the schematic diagram is shown in Fig. 2. R is the distance between the jammer and the radar being jammed, θ is the angle between jammer and the radar. Two LDs (Laser diodes) emit the continuous-wave optical carriers with different wavelengths of ω_1 and ω_2 , as well as different powers of P_1 and P_2, respectively.

The received radar signals are modulated to the MZMs (Mach-Zehnder modulators). The two MZMs are adjusted at the quadrature bias points. Assuming the radar signals modulated to MZM1 and MZM2 are $V_1\cos[\omega_s(t-\tau_1)]$ and $V_2\cos[\omega_s(t-\tau_2)]$, respectively. ω_s is the radar signal's angular frequency. V_1 and V_2 are the amplitude of the two radar signals, τ_1 and τ_2 are the transmission delay from monopulse radar to the two antennas, respectively. Under small signal modulation, the output optical fields of the two MZMs can be written as

$$E_1(t) \propto \sqrt{P_1}\exp(j\omega_1 t) \left\{ \begin{array}{l} J_0\left(\frac{m_1}{2}\right) \\ -J_1\left(\frac{m_1}{2}\right)\exp\left[j\omega_s(t-\tau_1)\right] \\ -J_1\left(\frac{m_1}{2}\right)\exp\left[-j\omega_s(t-\tau_1)\right] \end{array} \right\} \quad (1)$$

$$E_2(t) \propto \sqrt{P_2}\exp(j\omega_2 t) \left\{ \begin{array}{l} J_0\left(\frac{m_2}{2}\right) \\ -J_1\left(\frac{m_2}{2}\right)\exp\left[j\omega_s(t-\tau_2)\right] \\ -J_1\left(\frac{m_2}{2}\right)\exp\left[-j\omega_s(t-\tau_2)\right] \end{array} \right\} \quad (2)$$

where $m_1 = \pi V_1/V_\pi$ and $m_2 = \pi V_2/V_\pi$ are the modulation indices produced by the two radar signals. V_π is the half-wave voltage of the MZM.

An OSP is utilized to adjust the phase of $E_2(t)$. As shown in Fig. 2(b) and (c), the upper-sideband and lower-sideband of $E_2(t)$ are introduced with opposite phase shifts by the OSP. The output optical fields of the OSP can be expressed as

$$E_2(t) \propto \sqrt{P_2}\exp(j\omega_2 t) \left\{ \begin{array}{l} J_0\left(\frac{m_2}{2}\right) \\ -J_1\left(\frac{m_2}{2}\right)\exp\left[j\omega_s(t-\tau_2)+j\Delta\phi\right] \\ -J_1\left(\frac{m_2}{2}\right)\exp\left[-j\omega_s(t-\tau_2)-j\Delta\phi\right] \end{array} \right\} \quad (3)$$

where $\Delta\phi$ is the phase shift that can be tuned by programming the OSP. The two optical signals transmit through the fiber and then the PDs (photodetectors) beat the sidebands with the optical carriers and generate the jamming signals. The cross-eye jammer then emits the jamming signals to the radar being jammed. The two jamming signals received by the radar being jammed can be written as

$$I_1(t) \propto \Re_1\alpha_1 P_1 J_0\left(\frac{m_1}{2}\right) J_1\left(\frac{m_1}{2}\right) \cos\left[\omega_s\left(t-\tau_1-\tau_{CCW}-\tau_2\right)\right] \tag{4}$$

$$I_2(t) \propto \Re_2\alpha_2 P_2 J_0\left(\frac{m_2}{2}\right) J_1\left(\frac{m_2}{2}\right) \times \cos\left[\omega_s\left(t-\tau_2-\tau_{CW}-\tau_1\right)+\Delta\phi\right] \tag{5}$$

where τ_{CW} and τ_{CCW} are the transmission delays of the optical signals in clockwise and counterclockwise directions, respectively. α_1 and α_2 are the transmission losses of the two jamming signals, respectively. $\Re_1$ and $\Re_2$ are the responsivity of PD1 and PD2, respectively.

The angular error θ_e induced to the radars by the cross-eye jammer can be expressed as [22]:

$$\theta_e \approx \frac{d\cos\theta}{2R} G_C \tag{6}$$

Cross-eye gain G_C can be written as [22]:

$$G_C = \frac{1-a^2}{1+2a\cos(\Phi)+a^2} \tag{7}$$

where a is the relative amplitude and Φ is the phase difference of the two jamming signals.

To achieve high cross-eye gain and thus induce large angular error to the radar being jammed, a should be 1 and Φ should be π [17]. Thus, the OSP is programmed to adjust the phase difference between the two jamming signals to be π. The transmission delays of the two optical signals are also adjusted to be equal by finely tuning the length of the optical fiber. The relative amplitude of the two jamming signals is adjusted to be equal by tuning the power of the optical carriers. When the two jamming signals have equal magnitudes, opposite phases and matching time delays, the largest angular error can be achieved. The conditions for jamming can be expressed as

$$\Re_1\alpha_1 P_1 J_0\left(\frac{m_1}{2}\right) J_1\left(\frac{m_1}{2}\right) = \Re_2\alpha_2 P_2 J_0\left(\frac{m_2}{2}\right) J_1\left(\frac{m_2}{2}\right) \tag{8}$$

$$\Delta\phi = \pi \tag{9}$$

$$\tau_{CW} = \tau_{CCW} \tag{10}$$

However, these conditions are hard to be achieved due to the stability and the tuning accuracy of the system. The amplitude mismatch and phase mismatch between the transfer functions of CW and CCW paths are the key factors affecting the cross-eye gain. Fig. 3 shows the simulation result. It can be seen that the cross-eye gain is a strong function of the two parameters, and can be maximized with low mismatches.

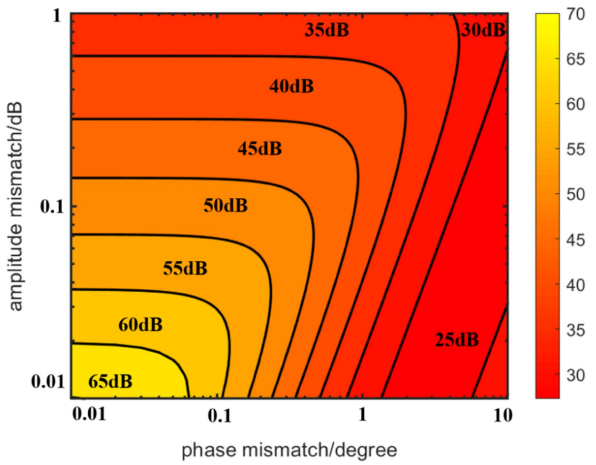

Fig. 3. Simulated cross-eye gain showing reliance on amplitude mismatch and phase mismatch.

The two jamming signals will distort the phase-front strongly and thus induce large angular error to the radar. The following simulation results show the effect of phase-front distortion caused by the cross-eye jammer. In the simulation, the frequency of the radar signal's carrier is 8 GHz, and the distance between the two jamming antennas is 10 m, the distance between the radar and the jammer is 30000 m. In the simulation, the jammer is in the direction of the tracking radar's boresight. The phase-fronts formed by the jamming signals under different parameters are shown in Fig. 4. Compared Fig. 4(a) with (b), the distortion of the phase-fronts will be more severe when the relative amplitude is closer to 1 and phase difference is closer to π. Thus larger angular error will be induced to the radar.

III. Experiment and Results

An experiment is carried out to verify the proposed novel cross-eye jammer. We built the experimental setup which is shown in Fig. 5. A vector network analyzer (VNA, Rohde &Schwarz, ZVA-67) is used to measure the transfer functions of CW and CCW paths. An Anristu's MT9812B tunable laser is used to emit optical carriers. By adjusting the intensity of the optical carrier and the transmission loss of the two paths, the amplitude of the jamming signals can be adjusted to be equal. The optical frequency of the two lasers are 193.8 THz and 194 THz. The two optical carriers drove the Fujitsu's FTM7938 MZMs with the half-voltage of 5 V and 3-dB bandwidth of 37 GHz. We use a Finisar's waveshaper16000S to realize optical phase inversion. After transmission through the optical fiber, the photoelectric conversion is realized by a PD with the bandwidth of 30 GHz. The time delay of the two paths are precisely matched by using an optical tunable delay line (TODL) with sub-picosecond resolution.

The CW and CCW paths' transfer functions of X band, Ku band and K band are obtained by using the VNA. The amplitude mismatch and phase difference between the two transfer functions can be obtained by comparing the two transfer functions. The experimental results are shown in Fig. 6. The two figures exhibit flat amplitude and uniform phase inversion over the

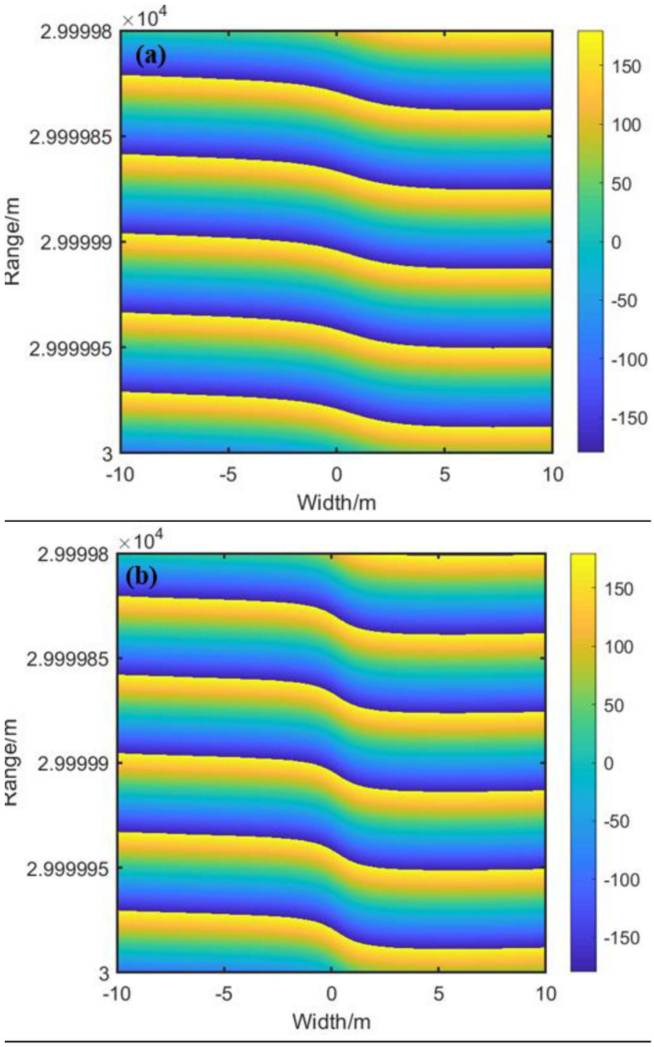

Fig. 4. Phase-front formed by the jamming signals when (a) $a = 0.9$, $\Phi = 182°$ and (b) $a = 0.95, \Phi = 181°$.

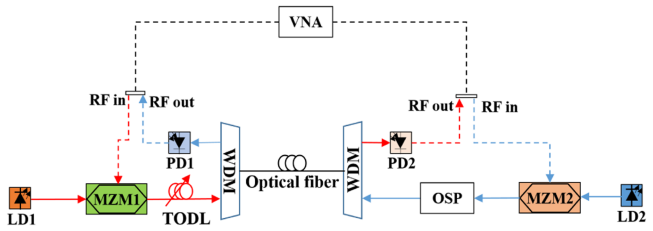

Fig. 5. Experimental setup for measuring the transfer functions of jammer's CW and CCW paths. VNA, vector network analyzer; TODL, tunable optical delay line; LD: Laser diode; OSP: Optical spectrum processor; MZM, Mach-Zehnder modulator; PD: Photodetector; WDM: Wavelength division multiplexer.

three bands. The maximum amplitude and phase mismatches between the transfer functions of CW and CCW paths are below 0.4 dB and 2.15 degrees, respectively. The root mean square of the amplitude mismatch of X-band, Ku-band and K-band is 0.14 dB, 0.07 dB and 0.15 dB. The root mean square of the phase mismatch of X-band, Ku-band and K-band is 1.02 degree, 0.65 degree and 0.65 degree. The experimental results show

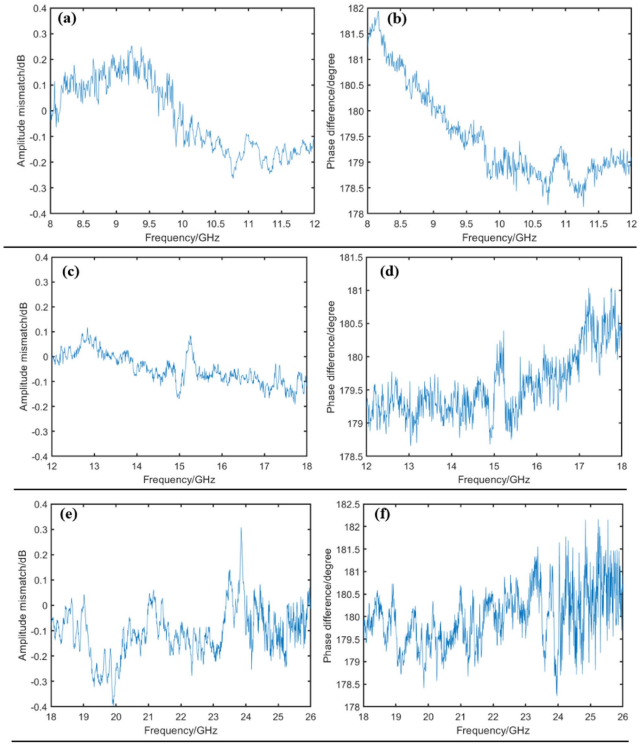

Fig. 6. Amplitude mismatch and phase difference between the transfer functions of CW path and CCW path. Experimental results of (a), (b) X band, (c), (d) Ku band and (e), (f) K band.

higher tuning accuracy in the case of high operating frequency and wide bandwidth compared with the technique proposed in [34]. Although the cost and complexity of the proposed system is more complex, it can achieve higher cross-eye gain. According to the discussion in last section, the proposed cross-eye jammer can realize over 39 dB of cross-eye gain. Large angular error can be induced to the tracking radar.

Flat-response transfer functions of the system have been achieved, which verifies broadband signal processing capability of the OSP. However, the uneven frequency response of the RF front-end may distort the performance of the system in practice. This issue can be solved by using broadband and flat-response RF front-end based on photonic technology [35]. Higher frequency and wider bandwidth can be realized by utilizing the PD with higher 3 dB bandwidth.

IV. Conclusion

A novel photonic-enabled broadband cross-eye jamming system is demonstrated in this paper. The novel cross-eye jammer utilizes the OSP to realize phase inversion, and thus generate two jamming signals. Simulations have been conducted to investigate the impact of mismatches on cross-eye gain. Furthermore, the phase-front distortion is simulated. In the experiments, we measure the transfer functions of the two paths in X, Ku and K band. Experimental results show that the amplitude mismatch and phase mismatch between the two paths are below 0.4 dB and 2.15 degrees, respectively. Calculated cross-eye gain is 39 dB. Due to its capability of generating broadband jamming

signals, the proposed scheme breaks the "electrical bottleneck" of traditional cross-eye systems and has the ability of jamming radars whose carrier frequency covers a large spectral range. The proposed cross-eye jamming system may be applied to future electrical warfare.

REFERENCES

[1] R. L. Fante, "Synthesis of adaptive monopulse patterns," *IEEE Trans. Antennas Propag.*, vol. 47, no. 5, pp. 773–774, May 1999.

[2] Y. Seliktar, E. J. Holder, and D. B. Williams, "An adaptive monopulse processor for angle estimation in a mainbeam jamming and coherent interference scenario," in *Proc. IEEE Int. Conf. Acoust. Speech Signal Process.*, 1998, pp. 2037–2040.

[3] R. Roy and T. Kailath, "ESPRIT-estimation of signal parameters via rotational invariance techniques," *IEEE Trans. Acoust., Speech, Signal Process.*, vol. 37, no. 7, pp. 984–995, Jul. 1989.

[4] Z. I. Khan, M. M. Kamal, N. Hamzah, K. Othman, and N. I. Khan, "Analysis of performance for multiple signal classification (MUSIC) in estimating direction of arrival," in *Proc. IEEE Int. Radio Freq. Microw. Conf.*, 2008, pp. 524–529.

[5] D. Kundu, "Modified MUSIC algorithm for estimating DOA of signals," *Signal Process.*, vol. 48, no. 1, pp. 85–90, 1996.

[6] J. Jo, J. Lee, and J. Ahn, "A study on the jamming technique for monopulse missile using TESS," *Proc. Korean Inst. Commun. Inf. Sci.*, vol. 63, 2017.

[7] Z. Wang, A. Sinha, P. Willett, and Y. Bar-Shalom, "Angle estimation for two unresolved targets with monopulse radar," *IEEE Trans. Aerosp. Electron. Syst.*, vol. 40, no. 3, pp. 998–1019, Jul. 2004.

[8] A. I. Leonov, "History of monopulse radar in the USSR," *IEEE Aerosp. Electron. Syst. Mag.*, vol. 13, no. 5, pp. 7–13, May 1998.

[9] İ. Kalinbacak, M. Pehlivan, and K. Yeğin, "Cross polarization monopulse jammer located on UAV," in *Proc. IEEE 8th Int. Conf. Recent Adv. Space Technol.*, 2017, pp. 337–341.

[10] H. Han, X. Xu, H. Wang, and H. Dai, "Analysis of cross-polarization jamming for phase comparison monopulse radars," in *Proc. IEEE 2nd Int. Conf. Electron. Inf. Commun. Technol.*, 2019, pp. 404–407.

[11] F. Neri, "Anti-monopulse jamming techniques," in *Proc. IEEE/SBMO Microw. Theory Technol. Soc. Int. Microw. Optoelectron. Conf.*, 2001, pp. 45–50.

[12] L. Bao et al., "Impact of cooperative jamming of dual stealth aircraft formation on detection performance of monopulse radar," *Amer. Inst. Phys. Adv.*, vol. 10, no. 12, 2020, Art. no. 125007.

[13] L. Bao et al., "Infuence of self-defense conherent jamming of dual stealth aircraft on monopulse radar with long-range support jamming," *Syst. Eng. Electron.*, vol. 41, no. 9, pp. 1973–1983, 2019.

[14] N. B Benton, "Fiber optic microwave link applications in towed decoy electronic countermeasure systems," *Opt. Technol. Microw. Appl. VII*, vol. 2560, pp. 85–92, 1995.

[15] S. Vardhan and A. Garg, "Information jamming in electronic warfare: Operational requirements and techniques," in *Proc. IEEE Int. Conf. Electron., Commun. Comput. Eng.*, 2014, pp. 49–54.

[16] S.-Y. Liu, C.-X. Dong, J. Xu, G.-Q. Zhao, and Y.-T. Zhu, "Analysis of rotating cross-eye jamming," *IEEE Antennas Wireless Propag. Lett.*, vol. 14, pp. 939–942, Dec. 2015.

[17] W. P. du Plessis, J. W. Odendaal, and J. Joubert, "Extended analysis of retrodirective cross-eye jamming," *IEEE Trans. Antennas Propag.*, vol. 57, no. 9, pp. 2803–2806, Sep. 2009.

[18] W. P. duPlessis, J. W. Odendaal, and J. Joubert, "Tolerance analysis of cross-eye jamming systems," *IEEE Trans. Aerosp. Electron. Syst.*, vol. 47, no. 1, pp. 740–745, Jan. 2011.

[19] T. Liu, D. Liao, X. Wei, and L. Li, "Performance analysis of multiple-element retrodirective cross-eye jamming based on linear array," *IEEE Trans. Aerosp. Electron. Syst.*, vol. 51, no. 3, pp. 1867–1876, Jul. 2015.

[20] W. D. Plessis, "Cross-eye gain in multiloop retrodirective cross-eye jamming," *IEEE Trans. Aerosp. Electron. Syst.*, vol. 52, no. 2, pp. 875–882, Apr. 2016.

[21] W. P. Du Plessis, "Platform skin return and retrodirective cross-eye jamming," *IEEE Trans. Aerosp. Electron. Syst.*, vol. 48, no. 1, pp. 490–501, Jan. 2012.

[22] W. P. Du Plessis, "A comprehensive investigation of retrodirective cross-eye jamming," Ph.D. dissertation, Univ. of Pretoria, Pretoria, South Africa, 2010.

[23] W. P. duPlessis, J. W. Odendaal, and J. Joubert, "Experimental simulation of retrodirective cross-eye jamming," *IEEE Trans. Aerosp. Electron. Syst.*, vol. 47, no. 1, pp. 734–740, Jan. 2011.

[24] F.-P. Pieterse and W. P. de Plessis, "Implementation and testing of a retrodirective cross-eye jammer," *IEEE Trans. Aerosp. Electron. Syst.*, vol. 58, no. 5, pp. 4486–4494, Oct. 2022.

[25] F. Neri, "Experimental testing on cross-eye jamming," in *Proc. AOC Int. Symp. Conf.*, 2000.

[26] L. Falk, "Cross-eye jamming of monopulse radar," in *Proc. IEEE Int. Waveform Diversity Des. Conf.*, 2007, pp. 209–213.

[27] W. P. du Plessis, "Practical implications of recent cross-eye jamming research," in *Proc. Defination Oper. Appl. Symp.*, 2012, pp. 167–174.

[28] X. Xiao et al., "A microwave photonics-based inverse synthetic aperture radar system," in *Proc. IEEE Conf. Lasers Electro-Opt.*, 2017, pp. 1–2.

[29] X. Ye, F. Zhang, Y. Yang, D. Zhu, and S. Pan, "Photonics-based high-resolution 3D inverse synthetic aperture radar imaging," *IEEE Access*, vol. 7, pp. 79503–79509, 2019.

[30] X. Ye, F. Zhang, Y. Yang, and S. Pan, "Photonics-based radar with balanced I/Q de-chirping for interference-suppressed high-resolution detection and imaging," *Photon. Res.*, vol. 7, pp. 265–272, 2019.

[31] Y. Yao, F. Zhang, Y. Zhang, X. Ye, D. Zhu, and S. Pan, "Demonstration of ultra-high-resolution photonics-based Kaband inverse synthetic aperture radar imaging," in *Proc. IEEE Opt. Fiber Commun. Conf. Expo.*, 2018, pp. 1–3.

[32] S. Peng, S. Li, X. Xue, X. Xiao, and X. Zheng, "Photonics-based simultaneous distance and velocity measurement of multiple targets utilizing dual-band symmetrical triangular linear frequency-modulated waveforms," *Opt. Exp.*, vol. 28, pp. 16270–16279, 2020.

[33] S. Peng, S. Li, X. Xue, X. Xiao, D. Wu, and X. Zheng, "A photonics-based coherent dual-band radar for super-resolution range profile," *IEEE Photon. J.*, vol. 11, no. 4, Aug. 2019, Art. no. 5502408.

[34] L. Yaron, T. Langer, Y. Geiler, S. Zach, and M. Tur, "Wideband $0/\pi$ retro-reflective photonic system," in *Proc. IEEE Int. Conf. Microw., Commun., Antennas Electron. Syst.*, 2011, pp. 1–4.

[35] S. Pan and Y. Zhang, "Microwave photonic radars," *J. Lightw. Technol.*, vol. 38, no. 19, pp. 5450–5484, Oct. 2020.